

Electronic Supplementary Information for:

**Designed Additive Suppresses Interpenetration in IRMOF-10**

Cassidy A. Carey,<sup>b</sup> Leila M. Foroughi,<sup>a</sup> and Adam J. Matzger<sup>\*a,b</sup>

<sup>a</sup>Department of Chemistry, University of Michigan, 930 North University Avenue, Ann Arbor, Michigan 48109, United States

<sup>b</sup>Macromolecular Science and Engineering Program, University of Michigan, Ann Arbor, MI 48019, United States

\*To whom correspondence should be addressed. Email address: matzger@umich.edu

**Table of Contents.**

S1. Materials

S2. Instrumental Details and Methods

S3. Synthesis

S4. Characterization

S5. Crystallographic Data

S6. Summary of Studies for IRMOF-9 and 10

S7. References

## S1. Materials

Diethylformamide (DEF, TCI America, 99%, purified by storage on activated charcoal for ~1 month followed by removal of impurities via silica gel column and distillation, stored over 4 Å sieves prior to use), zinc nitrate hexahydrate (Certified ACS, dried under vacuum ( $10^{-2}$  Torr) for 4 days at room temperature and stored in a desiccator prior to use), sodium chloride (certified ACS), potassium hydroxide (pellets, certified ACS), 1,4-dioxane (certified ACS), *N,N*-dimethylformamide (certified ACS, 99.8%, stored over 4 Å sieves prior to use), dichloromethane (certified ACS), hexane (Certified ACS), and hydrochloric acid (certified ACS Plus) were purchased from Fisher Chemical (Waltham, MA). Dimethylsulfoxide- $d_6$  (99.9% atom % D) and deuterium chloride solution (35wt% in  $D_2O$ , 99.9% atom % D) were purchased from Sigma-Aldrich. Tetrakis(triphenylphosphine)palladium(0) (99.9+% Pd) was purchased from Strem Chemicals. Potassium phosphate tribasic was purchased from Thermo Fisher Scientific. 1,3,5-Tribromobenzene (95+%) was purchased from Matrix Scientific. [1,1'-Biphenyl]-4,4'-dicarboxylic acid (97%) was purchased from Ark Pharma Scientific. 4'-(Methoxycarbonyl)-[1,1'-biphenyl]-4-yl)boronic acid (97%) was purchased from Ambeed.

## S2. Instrumental Details and Methods

### Powder X-ray diffraction:

Powder X-ray diffraction patterns were collected on a PANalytical Empyrean diffractometer at with a  $Cu K\alpha$  radiation ( $\lambda = 1.541874 \text{ \AA}$ ) tube operating 45 kV, 40 mA. MOF samples (coated in mineral oil or solvated in DMF) were loaded on a zero-background Si sample holder in air for analysis. The incident beam was equipped with a Bragg-Brentano HD X-ray optic and X-ray detection was accomplished with an X'Celerator Scientific Detector operating in continuous 1D scanning mode. Diffraction patterns were collected from 2 to  $50^\circ 2\theta$  with a scan step size of  $0.0084^\circ$  and 29.845 s step speed.

### Nitrogen sorption:

$N_2$  sorption experiments were performed on a NOVA e series 4200 surface area analyzer (Quantachrome Instruments, Boynton Beach, Florida, USA).  $N_2$  (99.999%) was purchased from Cryogenic Gases. For  $N_2$  measurements, a glass sample cell was charged with ~20 mg of sample in a nitrogen glove box and analyzed at 77 K.  $N_2$  sorption isotherms were collected in the NOVA-win software. Consistency criterion plots were used to determine the  $P/P_0$  range for BET surface area analysis. All MOFs were activated under flowing supercritical  $CO_2$ .

### Supercritical $CO_2$ Activation:

DMF solvated samples of IRMOF-9 and IRMOF-9/10 were activated by flowing supercritical  $CO_2$  according to a similar procedure.<sup>1</sup> Initially, samples were loaded into a stainless steel column and subjected to a  $CO_2$  flowrate of 2 mL/min for 2 hours at room temperature, then for 2 hours at  $55^\circ C$ . The flowrate was then decreased to 1 mL/min for the last hour of activation, and samples were loaded from the column into glass cells (for  $N_2$  sorption analysis) in a nitrogen glove box. The cells were sealed prior to loading onto the surface area analyzer.  $CO_2$  was purchased from Metro Welding Supply (Detroit, MI).

### MOF Digestion for NMR Analysis:

In a Teflon-lined screw cap 4 mL vial, 0.6 mg of activated MOF was added to 550  $\mu L$  of  $DMSO-d_6$ , 20  $\mu L$  of  $D_2O$ , and 25  $\mu L$  of  $DCl$ . The mixture was sonicated for 1 minute and heated at  $50^\circ C$  for 1 hour (or until dissolved) prior to NMR analysis.

### Single Crystal X-Ray Diffraction:

Single-crystal X-Ray diffraction data were collected on IRMOF-9/10 crystals exchanged in hexane using a Rigaku XtaLAB Synergy-S X-ray diffractometer in a kappa goniometer geometry configuration. The X-ray source is a PhotonJet-S microfocus Cu source ( $\lambda = 1.54187 \text{ \AA}$ ) operated at 50 kV and 1 mA. X-ray intensities were measured with a HyPix-6000HE detector held 34.00 mm from the sample. The data were processed using CrysAlisPro v42.75a (Rigaku Oxford Diffraction) and were corrected for absorption. The structure of IRMOF-10 was solved using and SHELXT<sup>2</sup> in OLEX2<sup>3</sup> and refined using SHELXL.<sup>4</sup> All non-hydrogen atoms were refined anisotropically with hydrogen atoms located at idealized positions. A mask was used to account for the electron density associated with disordered solvent molecules.

### Timelapse Collection:

MOF solutions were prepared according to section S3 and added to a 20 mL scintillation vial along with a grain of sand to focus the camera prior to collection. The Teflon lined cap was fitted with a custom glass insert to allow light to pass through. The capped vial was placed in a heated block set to 85 °C fixed above a half wave plate (S-APHW280P-096G-AR2-50X50MM, American Polarizers Inc.) and a Canon EOS 5DS R camera (DS126611) with a polarizing filter (heliopan Digital ES 58 Pol lin. 2.5 $\times$ ) attached to the Canon MP-E 65mm 1:2.8 1-5 $\times$  macro photo lens. A polarizing plate (S-AP42-100G-AR2-50X50MM, American Polarizers Inc.) was placed on top of the cap of the vial. A light was centered directly above the cap and images were automatically collected every 300 s during synthesis using DSLR Remote Pro software to monitor the crystallization under polarized light. Timelapses of the acquired images were created using ImageJ software.

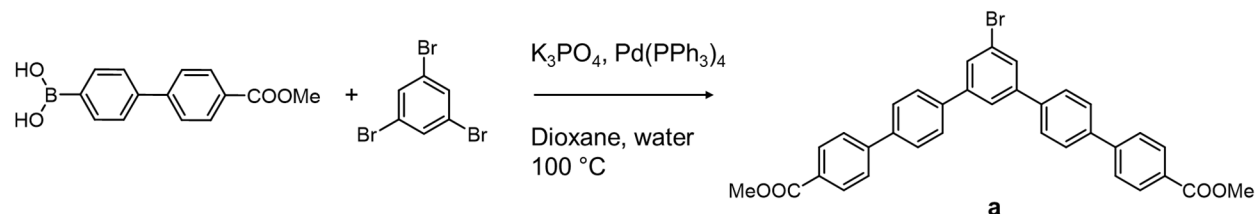
### MOF Pore Size Calculation:

The pore sizes of IRMOF-9 and IRMOF-10 were estimated in Mercury 2023.2.0 using the pore analyser calculation on the structures of IRMOF-9 (Refcode: EDUVAA)<sup>5</sup> and IRMOF-10 (Deposition Number: 2356184). Solvent was removed from the structures prior to pore size calculation.

### Additive Design:

Additive design was based on previous methodology<sup>6</sup> by matching the C-C distance of two carboxylates attached to two diagonally situated Zn clusters across a pore window of IRMOF-10 (measured in Mercury 2023.2.0) to the C-C distance (of the carboxylates) of the bent dicarboxylic acid additive (measured in Spartan'20 V1.1.4) to favor bridging of the metal clusters across the pore window (of the {100} plane) during crystal growth.

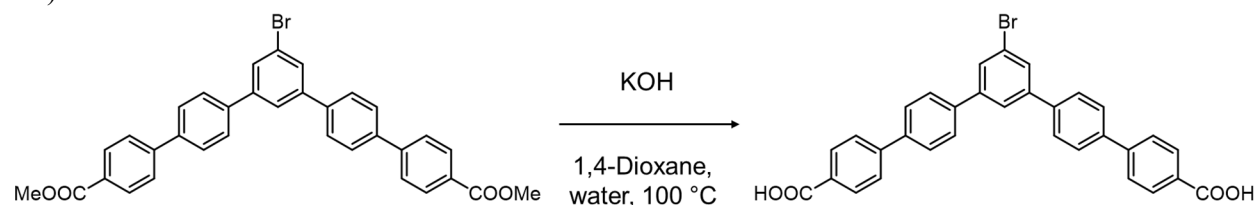
## S3. Synthesis



**Scheme S1.** Synthetic route for dimethyl 5-bromo-[1,1':4',1'':3'',1''':4''',1''':4''',1''':4''']-quinquephenyl]-4,4''-dicarboxylate (intermediate a).

### Intermediate a synthesis:

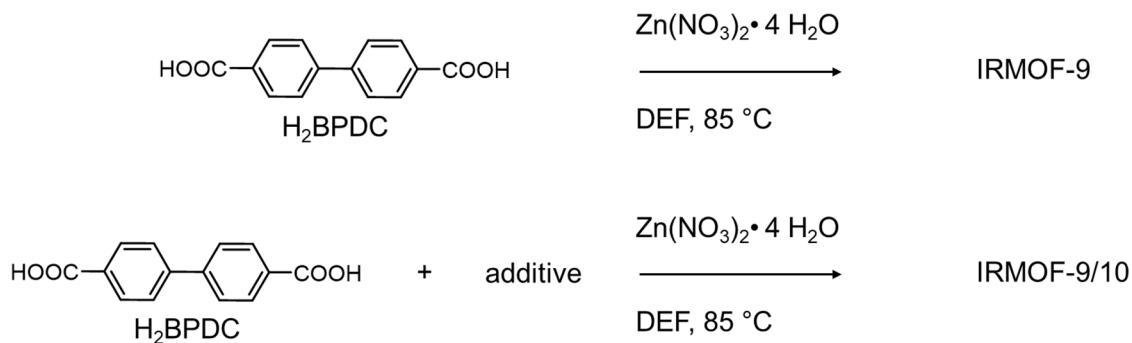
To a 150 mL pressure vessel, 67 mL of 1,4-dioxane was added and sparged with N<sub>2</sub>. After 30 minutes, 1,3,5-tribromobenzene (1.78 g, 5.65 mmol), and (4'-(methoxycarbonyl)-[1,1'-biphenyl]-4-yl)boronic acid (2.90 g, 11.3 mmol) were added to the sparging solution. After 10 minutes, K<sub>3</sub>PO<sub>4</sub> (7.19 g, 33.9 mmol) and 5.3 mL of DI water were added and sparged for an additional 20 minutes. Finally, tetrakis(triphenylphosphine) palladium(0) (161 mg, 0.139 mmol) was quickly added to the solution and the headspace of the vessel was backfilled with N<sub>2</sub> before capping. The vessel was stirred at 100 °C for 48 hours and then removed from heat to cool to room temperature. The reaction mixture was slowly added to 300 mL of DI water and stirred for 30 minutes. The resulting light brown precipitate was washed with DI water and collected by vacuum filtration and dried. The solids were then dissolved in 50 mL of DCM and the organic layer was extracted 2× with DI water and then once with brine. The organic layer was dried over MgSO<sub>4</sub> and coated onto silica. The product was isolated by flash column chromatography on a CombiFlash® RF+ automated flash chromatography system with a DCM/hexanes mobile phase. The second fraction (eluted at 3:1 DCM:Hexanes) was concentrated via rotary evaporation and recrystallized from hexanes to yield 720 mg of intermediate **a** as a white powder (bicoupled product yield: 22%). <sup>1</sup>H NMR (400 MHz, CD<sub>3</sub>Cl): δ 8.15-8.13 (d, 4H), 7.80 (m, 1H), 7.78 (m, 2H), 7.74-7.71 (m 12H), 3.96 (s, 6H).



**Scheme S2.** Synthetic route for 5-bromo-[1,1':4',1'':3'',1''':4''',1''''-quinquephenyl]-4,4''''-dicarboxylic acid.

### Additive synthesis:

To a 50 mL beaker, dimethyl 5-bromo-[1,1':4',1'':3'',1''':4''',1''''-quinquephenyl]-4,4''''-dicarboxylate (720 mg, 1.25 mmol) was added to 20 mL of 1,4-dioxane and stirred until dissolved. In a 100 mL round bottom flask, KOH (750 mg, 13.4 mmol) was dissolved in 20 mL of water. The dioxane solution was then added to the basic solution in the RBF and the mixture was stirred for 24 h at 100 °C. The contents of the flask were allowed to cool to room temperature and the solution was titrated with concentrated HCl until a pH ~3 was reached. The resulting white precipitate was washed with DI water, collected by filtration, and then dried under vacuum overnight. <sup>1</sup>H NMR (400 MHz, DMSO-D<sub>6</sub>): δ 12.99 (OH, s, 1H), 8.06-8.04 (m, 5H), 7.99-7.95 (m, 6H), 7.90-7.87 (dd, 8H).



**Scheme S3.** Synthetic route for IRMOF-9 and IRMOF-9/10.

#### IRMOF-9 Synthesis:

In a Teflon-lined screw cap scintillation vial,  $\text{Zn}(\text{NO}_3)_2 \cdot 4\text{H}_2\text{O}$  (109 mg, 0.42 mmol) and biphenyl-4,4'-dicarboxylic acid ( $\text{H}_2\text{BPDC}$ ) (13.7 mg, 0.057 mmol) were dissolved in 10 mL DEF via sonication for 30-40 min until dissolved. The solution was filtered through a 0.45  $\mu\text{m}$  syringe filter and was dispensed into a 20-mL Teflon-lined screw cap scintillation vial; the reaction was carried out in a DX 302 Yamato oven at 85 °C for 18 h. The product was repeatedly exchanged with DMF to remove unreacted starting material.

#### IRMOF-9/10 Synthesis:

In a Teflon-lined screw cap scintillation vial,  $\text{Zn}(\text{NO}_3)_2 \cdot 4\text{H}_2\text{O}$  (109 mg, 0.42 mmol), 5''-bromo-[1,1':4,1'':3'',1''':4''',1''''-quinquephenyl]-4,4''''-dicarboxylic acid (3.5 mg, 0.0064 mmol) and  $\text{H}_2\text{BPDC}$  (13.7 mg, 0.057 mmol) were dissolved in 10 mL DEF via sonication for 30-40 min until dissolved. The solution was filtered through a 0.45  $\mu\text{m}$  syringe filter and was dispensed into a 20-mL Teflon-lined screw cap scintillation vial; the reaction was carried out in a DX 302 Yamato oven at 85 °C for 18 h. The product was repeatedly exchanged with DMF to remove unreacted starting material.

#### IRMOF-9/10 (Early reaction analysis):

In a Teflon-lined screw cap scintillation vial,  $\text{Zn}(\text{NO}_3)_2 \cdot 4\text{H}_2\text{O}$  (109 mg, 0.42 mmol), 5''-bromo-[1,1':4,1'':3'',1''':4''',1''''-quinquephenyl]-4,4''''-dicarboxylic acid (3.5 mg, 0.0064 mmol) and  $\text{H}_2\text{BPDC}$  (13.7 mg, 0.057 mmol) were dissolved in 10 mL DEF via sonication for 30-40 min until dissolved. The solution was filtered through a 0.45  $\mu\text{m}$  syringe filter and was dispensed into a 20-mL Teflon-lined screw cap scintillation vial with a custom glass-windowed cap; the reaction was carried out in a heated block set 85 °C until the initial onset of birefringence was observed and then stopped (2-6 h, see Figure S7c for representative image). The product was repeatedly exchanged with DMF to remove unreacted starting material.

#### **S4. Characterization**

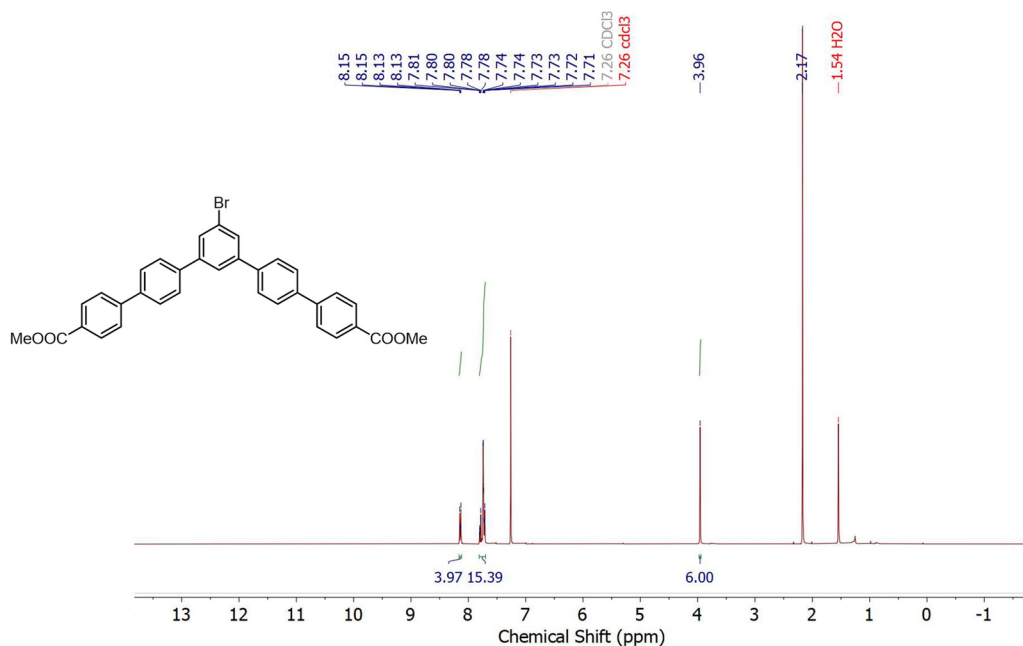


**Figure S1.**  $^1\text{H-NMR}$  spectrum of dimethyl 5''-bromo-[1,1':4,1'':3'',1''':4''',1''''-quinquephenyl]-4,4''''-dicarboxylate dissolved in  $\text{CD}_3\text{Cl}$  acquired with a 400 MHz Varian spectrometer.

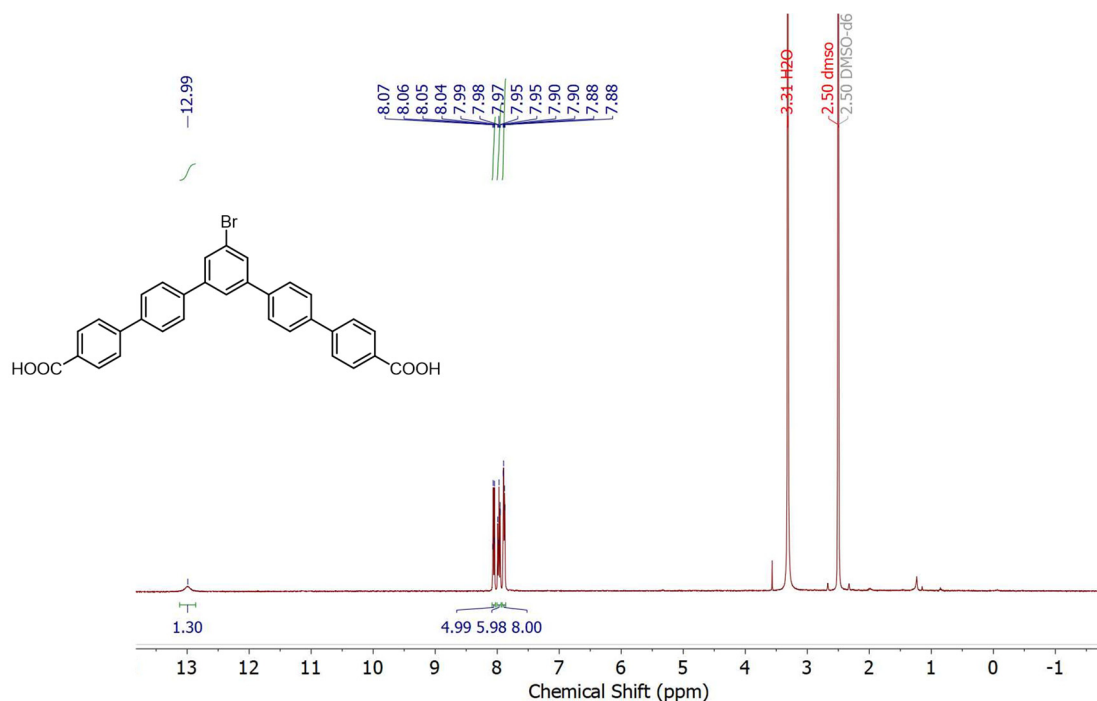


**Figure S2.** <sup>1</sup>H-NMR spectrum of 5''-bromo-[1,1':4',1'':3'',1''':4''',1''''-quinquephenyl]-4,4''''-dicarboxylic acid dissolved in DMSO-D<sub>6</sub> acquired with a 400 MHz Varian spectrometer.

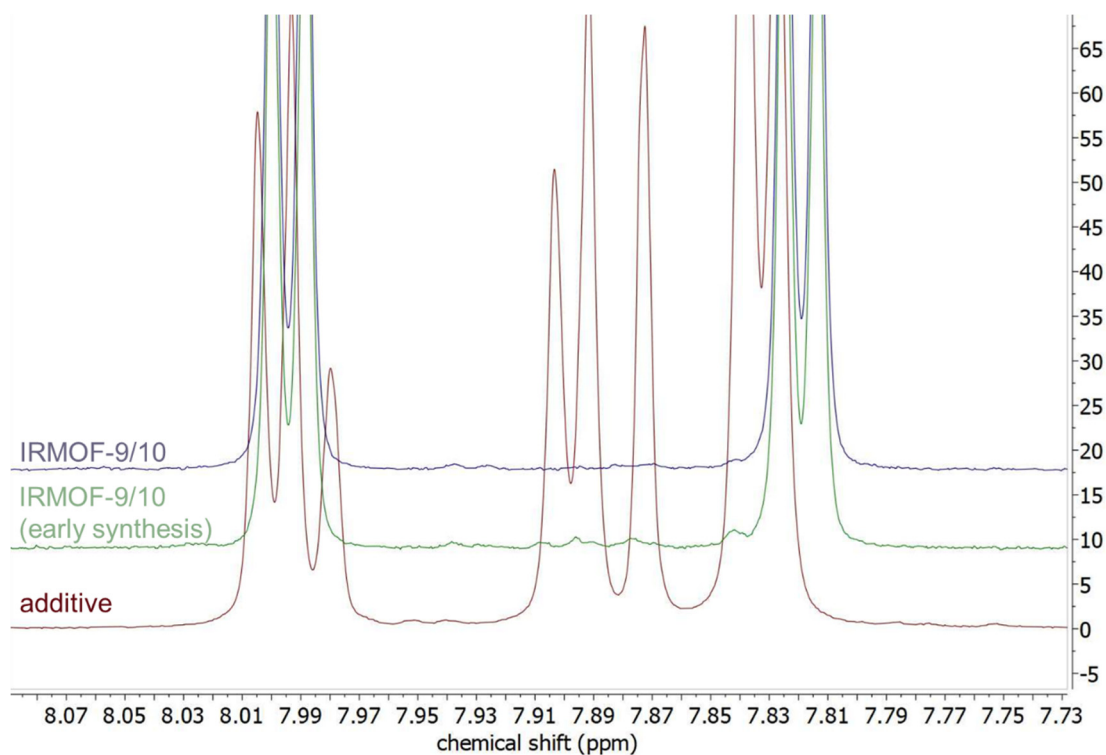


**Figure S3.** <sup>1</sup>H-NMR spectra of 5''-bromo-[1,1':4',1'':3'',1''':4''',1''''-quinquephenyl]-4,4''''-dicarboxylic acid (maroon), activated IRMOF-9/10 (early synthesis, green), and activated IRMOF-9/10 (grey). All samples were digested in DMSO-d<sub>6</sub>/D<sub>2</sub>O/DCI solution and acquired with a 700 MHz Varian spectrometer.

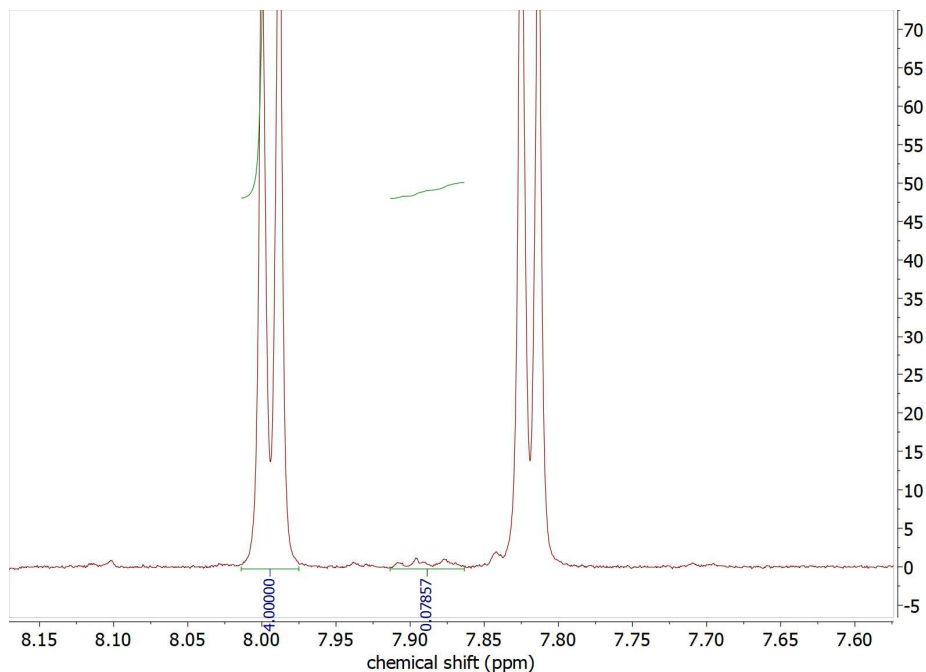


**Figure S4.**  $^1\text{H-NMR}$  spectra of IRMOF-9/10 (early synthesis) after activation. The sample was digested in  $\text{DMSO-d}_6/\text{D}_2\text{O}/\text{DCl}$  solution and acquired with a 700 MHz Varian spectrometer. Peaks at 7.99-8.00 ppm correspond to 4H from the linker and peaks at 7.86-7.91 ppm correspond to 6H from the additive. In this sample, additive peaks were observed at 1 mol %.

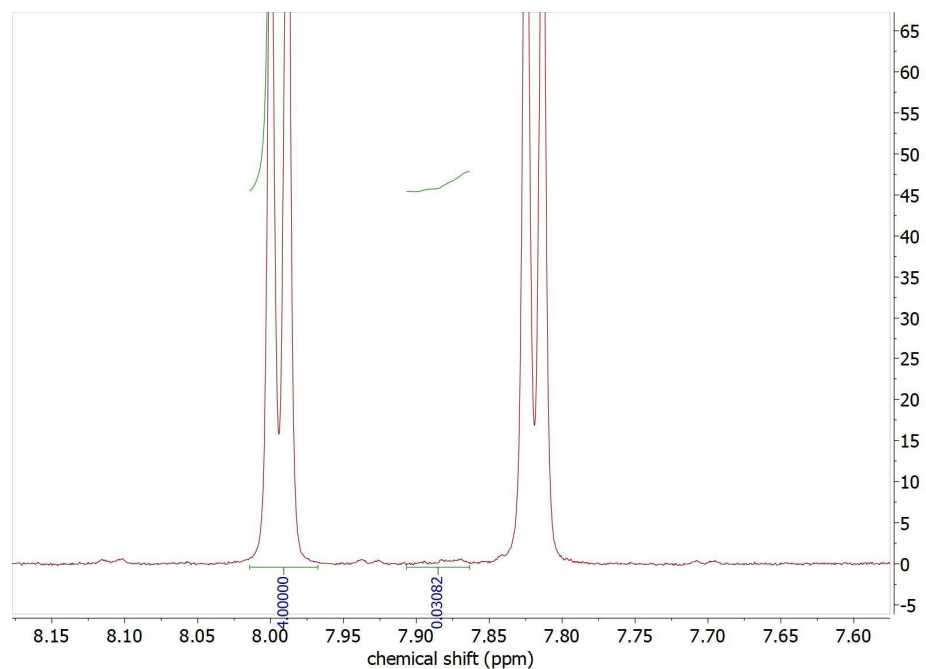


**Figure S5.**  $^1\text{H-NMR}$  spectra of IRMOF-9/10 after activation. The sample was digested in  $\text{DMSO-d}_6/\text{D}_2\text{O}/\text{DCl}$  solution and acquired with a 700 MHz Varian spectrometer. Peaks at 7.99-8.00 ppm correspond to 4H from the linker and peaks at 7.86-7.91 ppm correspond to 6H from the additive. In this sample, additive peaks were observed at <1 mol %.

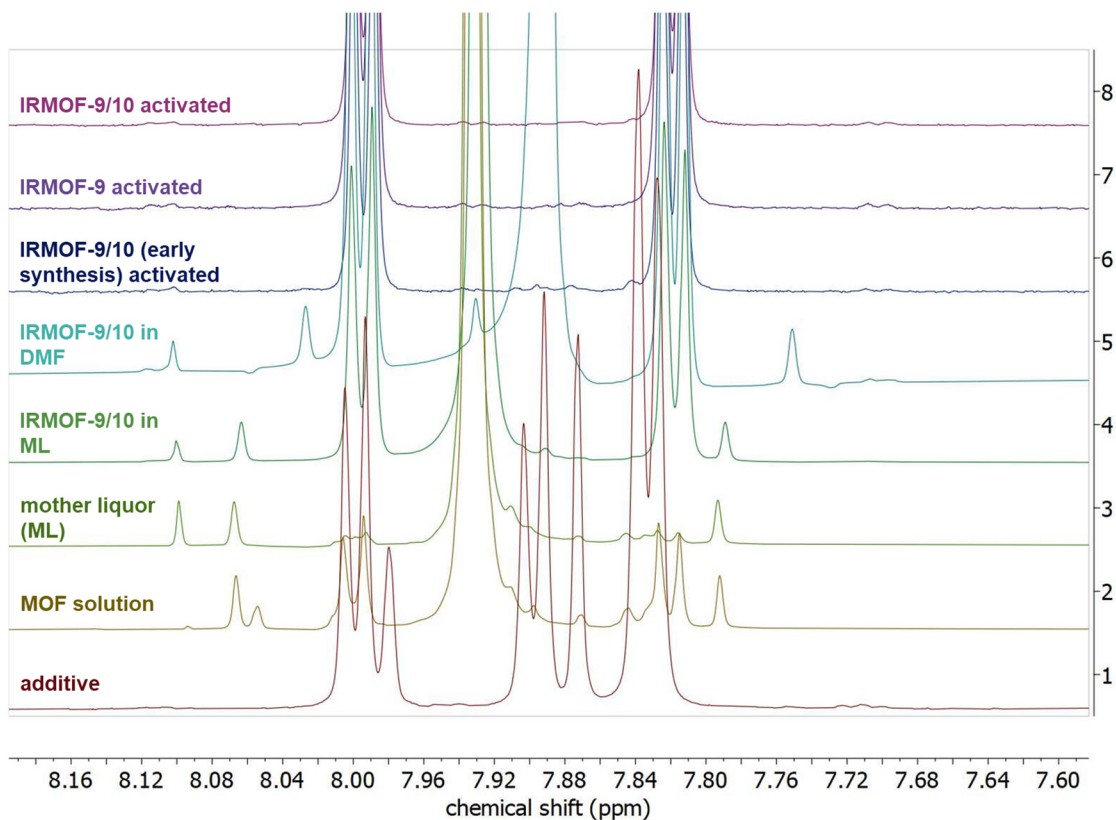


**Figure S6.**  $^1\text{H}$ -NMR spectra of the additive, MOF solution (prior to synthesis), mother liquor (ML), IRMOF-9/10 solvated in ML, IRMOF-9/10 after first exchange with DMF, IRMOF-9/10 (early synthesis) after activation, IRMOF-9 after activation, and IRMOF-9/10 after activation. Samples were digested or run directly in  $\text{DMSO-d}_6/\text{D}_2\text{O}/\text{DCI}$  solutions and acquired with a 700 MHz Varian spectrometer.

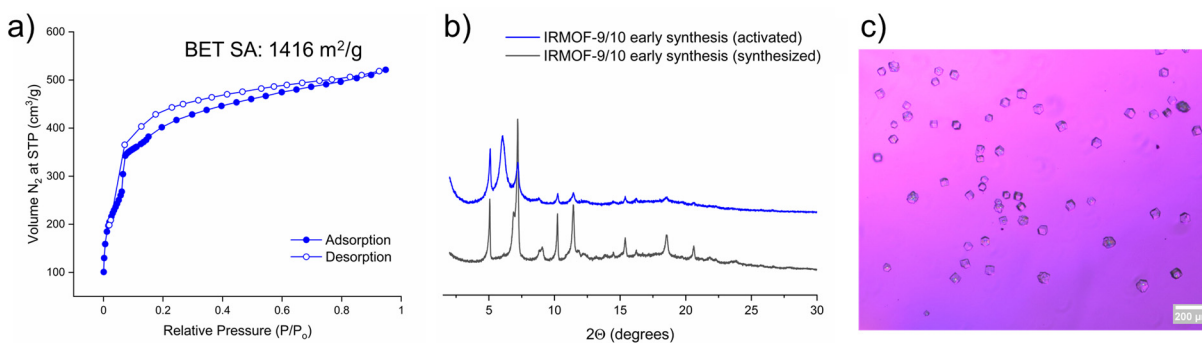


**Figure S7.** a)  $\text{N}_2$  adsorption isotherm for IRMOF-9/10 (early synthesis) crystals after activation with supercritical  $\text{CO}_2$ . b) Powder X-ray patterns of IRMOF-9/10 (early synthesis) crystals before (grey) and after activation (blue). c) Image of IRMOF-9/10 (early synthesis) crystals.



## S5. Crystallographic Data

Table S1: Crystallographic Data for IRMOF-10 (Deposition number: 2356184).

Formula	C <sub>42</sub> H <sub>24</sub> O <sub>13</sub> Zn <sub>4</sub>
Formula weight (g/mol)	998.09
Crystal system	cubic
Space group	<i>Fm</i> $\bar{3}$ <i>m</i>
Temperature (K)	293(2)
a = b = c (Å)	34.3966(2)
$\alpha = \beta = \gamma$ (°)	90
Volume (Å <sup>3</sup> )	40695.5(7)
Z	8
Z'	0.041667
$\rho_{\text{calc}}$ (g/cm <sup>3</sup> )	0.326
R <sub>1</sub> /wR <sub>2</sub> (all data)	0.0265/0.0734
Goof	1.014
Reflections collected	11527
Independent reflections	1824
R <sub>int</sub>	0.0210

## S6. Summary of Studies for IRMOF-9 and 10

Table S2: <sup>+</sup>crystal structure determined via single crystal X-ray diffraction, <sup>a</sup>volumetric surface area reported in m<sup>2</sup>/cm<sup>3</sup>, <sup>b</sup>pore aperture diameter, <sup>c</sup>internal pore diameter, <sup>d</sup>pore limiting diameter, <sup>e</sup>maximum pore diameter, <sup>f</sup>network accessible surface area

Material	Crystal System	Space Group	Activation method	Surface Area (m <sup>2</sup> /g)	Pore Diameter (Å)	Pore volume (cm <sup>3</sup> /g)	Reference
<b>Experimental Studies</b>							
IRMOF-9 <sup>+</sup>	orthorhombic	<i>Pn</i> <i>nm</i>	DCM	1904	-	0.90	5,7
IRMOF-9	orthorhombic	<i>Pn</i> <i>nm</i>	DCM	1168	9.9	-	8
IRMOF-10	cubic	<i>Fm</i> $\bar{3}$ <i>m</i>	DCM, CO <sub>2</sub>	478, 1778	14.9	-	8
IRMOF-9/10 <sup>+</sup>	cubic/ orthorhombic	<i>Fm</i> $\bar{3}$ <i>m</i> / <i>Pn</i> <i>nm</i>	CO <sub>2</sub>	2369	-	-	This work
IRMOF-9	orthorhombic	<i>Pn</i> <i>nm</i>	CO <sub>2</sub>	1964	-	-	This work
IRMOF-9	orthorhombic	<i>Pn</i> <i>nm</i>	CHCl <sub>3</sub>	1918 <sup>a</sup>	5.8, 8	1.18	9
$\alpha$ -IRMOF-9[dmf] <sup>+</sup>	orthorhombic	<i>Pn</i> <i>nm</i>	-	-	-	-	10
<b>Theoretical Studies</b>							
IRMOF-9	orthorhombic	<i>Pn</i> <i>nm</i>	-	2769 <sup>f</sup>	8.21 <sup>d</sup> , 11.02 <sup>e</sup>	0.96	This work
IRMOF-10	cubic	<i>Fm</i> $\bar{3}$ <i>m</i>	-	4913 <sup>f</sup>	12.03 <sup>d</sup> , 20.94 <sup>e</sup>	2.69	This work
IRMOF-9	orthorhombic	<i>Pn</i> <i>nm</i>	-	-	8.14 <sup>b</sup> , 11.0 <sup>c</sup>	-	8
IRMOF-10	cubic	<i>Fm</i> $\bar{3}$ <i>m</i>	-	-	11.65 <sup>b</sup> , 20.78 <sup>c</sup>	-	8
IRMOF-9	orthorhombic	<i>Pn</i> <i>nm</i>	-	4017	4.6/6.5/8.3/ 10.8	-	11
IRMOF-10	cubic	<i>Fm</i> $\bar{3}$ <i>m</i>	-	4970	16.7/20.2	-	11

## S7. References

- (1) Liu, B.; Wong-Foy, A. G.; Matzger, A. J. Rapid and Enhanced Activation of Microporous Coordination Polymers by Flowing Supercritical CO<sub>2</sub>. *Chem. Commun.* **2013**, 49 (14), 1419–1421. <https://doi.org/10.1039/C2CC37793D>.
- (2) Sheldrick, G. M. SHELXT – Integrated Space-Group and Crystal-Structure Determination. *Acta Crystallogr. Sect. Found. Adv.* **2015**, 71 (1), 3–8. <https://doi.org/10.1107/S2053273314026370>.
- (3) Dolomanov, O. V.; Bourhis, L. J.; Gildea, R. J.; Howard, J. a. K.; Puschmann, H. OLEX2: A Complete Structure Solution, Refinement and Analysis Program. *J. Appl. Crystallogr.* **2009**, 42 (2), 339–341. <https://doi.org/10.1107/S0021889808042726>.
- (4) Sheldrick, G. M. Crystal Structure Refinement with SHELXL. *Acta Crystallogr. Sect. C Struct. Chem.* **2015**, 71 (1), 3–8. <https://doi.org/10.1107/S2053229614024218>.
- (5) Eddaoudi, M.; Kim, J.; Rosi, N.; Vodak, D.; Wachter, J.; O’Keeffe, M.; Yaghi, O. M. Systematic Design of Pore Size and Functionality in Isoreticular MOFs and Their Application in Methane Storage. *Science* **2002**, 295 (5554), 469–472. <https://doi.org/10.1126/science.1067208>.
- (6) Suresh, K.; Kalenak, A. P.; Sotuyo, A.; Matzger, A. J. Metal–Organic Framework (MOF) Morphology Control by Design. *Chem. – Eur. J.* **2022**, 28 (18), e202200334. <https://doi.org/10.1002/chem.202200334>.
- (7) Rowsell, J. L. C.; Yaghi, O. M. Effects of Functionalization, Catenation, and Variation of the Metal Oxide and Organic Linking Units on the Low-Pressure Hydrogen Adsorption Properties of Metal–Organic Frameworks. *J. Am. Chem. Soc.* **2006**, 128 (4), 1304–1315. <https://doi.org/10.1021/ja056639q>.
- (8) Crom, A. B.; Strozier, J. L.; Tatebe, C. J.; Carey, C. A.; Feldblyum, J. I.; Genna, D. T. Deinterpenetration of IRMOF-9. *Chem. – Eur. J.* **2023**, 29 (70), e202302856. <https://doi.org/10.1002/chem.202302856>.
- (9) Babarao, R.; J. Coghlan, C.; Rankine, D.; M. Bloch, W.; K. Gransbury, G.; Sato, H.; Kitagawa, S.; J. Sumbly, C.; R. Hill, M.; J. Doonan, C. Does Functionalisation Enhance CO<sub>2</sub> Uptake in Interpenetrated MOFs? An Examination of the IRMOF-9 Series. *Chem. Commun.* **2014**, 50 (24), 3238–3241. <https://doi.org/10.1039/C4CC00700J>.
- (10) Canossa, S.; Pelagatti, P.; Bacchi, A. Drinking and Breathing: Solvent Coordination-Driven Plasticity of IRMOF-9. *Isr. J. Chem.* **2018**, 58 (9–10), 1131–1137. <https://doi.org/10.1002/ijch.201800061>.
- (11) Düren, T.; Millange, F.; Férey, G.; Walton, K. S.; Snurr, R. Q. Calculating Geometric Surface Areas as a Characterization Tool for Metal–Organic Frameworks. *J. Phys. Chem. C* **2007**, 111 (42), 15350–15356. <https://doi.org/10.1021/jp074723h>.